

Age-Dependent Modes of Extensional Necking Instability in Soft Glassy Materials

David M. Hoyle and Suzanne M. Fielding*

Department of Physics, Durham University, Science Laboratories, South Road, Durham DH1 3LE, United Kingdom

(Received 10 December 2014; published 15 April 2015)

We study the instability to necking of an initially cylindrical filament of soft glassy material subject to extensional stretching. By numerical simulation of the soft glassy rheology model and a simplified fluidity model, and by analytical predictions within a highly generic toy description, we show that the mode of instability is set by the age of the sample relative to the inverse of the applied extensional strain rate. Young samples neck gradually via a liquidlike mode, the onset of which is determined by both the elastic loading and plastic relaxation terms in the stress constitutive equation. Older samples fail at smaller draw ratios via a more rapid mode, the onset of which is determined only by the solidlike elastic loading terms (though plastic effects arise later, once appreciable necking develops). We show this solidlike mode to be the counterpart, for elastoplastic materials, of the Considère mode of necking in strain-rate-independent solids.

DOI: 10.1103/PhysRevLett.114.158301

PACS numbers: 83.60.Wc, 83.10.-y, 83.50.Jf, 83.80.-k

Many soft materials, including foams, emulsions, microgels, and colloids comprise disordering packings of mesoscopic substructures: foam bubbles, emulsion droplets, etc. At high volume fractions, the local rearrangement dynamics of these are impeded by large energy barriers and show a glassy slowing down. This underpins many universal features in the rheological (deformation and flow) properties of these “soft glassy materials” (SGMs). Particularly striking is the phenomenon of rheological ageing, in which an initially liquidlike sample slowly evolves towards an ever more solidlike state as a function of the time since it was prepared. In the last decade, significant progress has been made in understanding the role of ageing in the shear flow of SGMs [1]. Similar phenomena have been explored in polymeric [2] and metallic [3] glasses, with many unifying features across all these amorphous, elastoplastic materials.

Much less is understood about the response of these materials to extensional deformations, which are important to industrial processes in fiber spinning, ink-jetting, porous media, and the peeling and tack of surfaces bonded by adhesives. In the standard experimental test, an initially near uniform cylindrical (or rectangular) sample is steadily drawn out in length, with the aim of measuring the tensile stress as a function of strain and strain rate. Ubiquitously observed, however, is an instability to neck formation: the sample thins more quickly in the middle than at its end points (Fig. 1) and eventually fails. This has been observed in emulsions [4–8], laponite suspensions, [8–10], foams [11–13], polymer glasses [14,15], simulations of shear transformation zone models [16,17], and in shear thickening colloids [18–21] (though our focus here is on shear thinning SGMs).

A hallmark of all these elastoplastic materials is that their deformation properties depend strongly on the *rate* at which strain is applied, particularly when ageing is

present. For rate-independent materials, the onset of necking was predicted by Considère in 1885 [22] to coincide with a regime of declining tensile force as a function of strain. But despite the accumulating body of observations described above, counterpart criteria for necking in elastoplastic materials remain lacking (though for an insightful early study of rate dependence, see [23]). The contribution of this Letter is to provide such criteria, in the form of general analytical results supported by numerical simulation of two widely used models of soft glasses. In this way, we argue these new criteria to apply universally across all ageing elastoplastic materials and so to have the same, highly general status as the Considère criterion for rate-independent solids.

Importantly, we find the mode of instability to necking to be determined by the age t_w of the sample, relative to the inverse of the applied extensional (Hencky) strain rate $\dot{\epsilon}$: young samples ($\dot{\epsilon}t_w \ll 1$) fail by a gradual, liquidlike mode, whereas old samples ($\dot{\epsilon}t_w \gg 1$) show a fast, solidlike failure mode. We further show this solidlike mode to be the counterpart for elastoplastic materials of the Considère mode in rate-independent solids. In this way, crucially, the

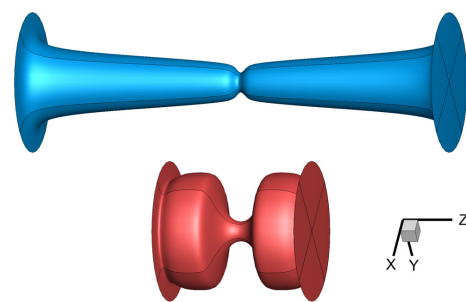


FIG. 1 (color online). Necked profiles. Extension rate shown by arrow in Fig. 2. Top: young sample, $t_w = 10^2$. Bottom: old, $t_w = 10^4$.

physics of a material's failure is predicted to be governed by a switch between two qualitatively distinct modes of instability, governed simply by the sample age [24].

We consider incompressible, inertialess deformations for which the velocity and stress fields in the material, $\mathbf{v}(\mathbf{r}, t)$ and $\mathbf{T}(\mathbf{r}, t)$, obey standard conditions of mass balance, $\nabla \cdot \mathbf{v} = 0$, and force balance, $\nabla \cdot \mathbf{T} = 0$. The total stress $\mathbf{T} = \Sigma + 2\eta\mathbf{D} - p\mathbf{I}$ comprises an elastoplastic contribution Σ from the mesoscopic substructures, a Newtonian solvent contribution of viscosity η , and an isotropic pressure. Here $K_{\alpha\beta} = \partial_\beta v_\alpha$ and $\mathbf{D} = \frac{1}{2}(\mathbf{K} + \mathbf{K}^T)$.

For the dynamics of the elastoplastic stress Σ we adopt the soft glassy rheology (SGR) model [25]. This considers an ensemble of elements, each corresponding to a local mesoscopic region of material. Under an imposed deformation, each element experiences a buildup of local elastic stress, intermittently released by plastic relaxation events. The treatment of tensorial stresses [26] within SGR was inspired by the Doi-Ohta model of dense emulsions [27], and considers a local density function $f(\mathbf{n})$ for the area (per unit volume) of droplet interfaces normal to \mathbf{n} , with a spherical normalization $Q = \int d\mathbf{n}f(\mathbf{n})$ and stress $\Sigma = G \int d\mathbf{n}(\mathbf{nn} - \frac{1}{3}\mathbf{I})f(\mathbf{n})$. The constant modulus $G = 1$ sets our stress scale. The buildup of elastic stress in any element during deformation obeys [27]

$$\begin{aligned} (\partial_t + \mathbf{v} \cdot \nabla)\Sigma &= \Sigma \cdot \mathbf{K} + \mathbf{K}^T \cdot \Sigma + \frac{2}{3}Q\mathbf{D} - \Sigma : \mathbf{K} \left(\frac{2}{3}\mathbf{I} + \frac{\Sigma}{Q} \right), \\ (\partial_t + \mathbf{v} \cdot \nabla)Q &= \mathbf{K} : \Sigma. \end{aligned} \quad (1)$$

Relaxation of stress by local plastic yielding events is modeled as hopping of the elements over strain-modulated energy barriers, governed by a noise temperature x . Upon yielding, any element resets its local stress to zero and selects its new energy barrier at random from an exponential distribution. This distribution confers a broad spectrum of yielding times $P(\tau)$, resulting in a glass phase with a yield stress for $x < 1$. Full details of the model in its original, spatially uniform form are in Refs. [25,26], and in its adaptation to spatially nonuniform shear flows in Ref. [28]. The counterpart adaptation for nonuniform extension is summarized in Ref. [29].

Because the SGR model is numerically rather cumbersome, we shall also present results for a simplified fluidity model in which SGR's full spectrum of yield times $P(\tau)$ is replaced by a single characteristic relaxation time scale τ . The right-hand side of Eqs. (1) then acquire relaxation terms: $-(1/\tau)Q\Sigma$ and $-(1/\tau)\mu Q^2$ for the Σ and Q dynamics, respectively. Here μ is a phenomenological parameter with $0 \leq \mu \leq 1$ [27]. A standard "fluidity" model for the dynamics of τ ,

$$(\partial_t + \mathbf{v} \cdot \nabla)\tau = 1 - \sqrt{2\mathbf{D}:\mathbf{D}}(\tau - \tau_0), \quad (2)$$

then captures the two essential ingredients of the SGR model: (i) ageing without flow, in which the relaxation time increases with the time since sample preparation, $\tau \sim t$; and (ii) rejuvenation by flow, which restores a steady state with $\tau = \tau_0 + 1/\sqrt{2\text{Tr}\mathbf{D}:\mathbf{D}}$. We choose units in which the microscopic time $\tau_0 = 1$.

We consider an initially cylindrical sample of length L_0 and radius R_0 , freshly prepared at time $t = 0$ in a fluidized state with $\tau = \tau_0$ and $\Sigma = \mathbf{0}$. It is then left to age undisturbed during a time $t_w \gg \tau_0$, before being steadily drawn out such that for times $t > t_w$ the length increases as $\dot{L} = \bar{\epsilon}(t)L$, with the cross sectional area correspondingly thinning. We present results below for two common protocols: (a) constant rate of Hencky strain $\bar{\epsilon}$, corresponding to $L = L_0 \exp[\bar{\epsilon}(t - t_w)]$, and (b) constant rate \dot{L} of length increase, corresponding to a progressively declining strain rate $\bar{\epsilon} = (1/\bar{\epsilon}_0 + t - t_w)^{-1}$.

For convenience, we solve the models within an one-dimensional (1D) approximation [29–31], in which the wavelengths of any variations that develop along the filament are assumed long compared to the radius. This standard assumption [32–34] has been shown to perform surprisingly well even some way into the regime where the wavelengths become comparable to the radius. It allows the neglect of any radial dependencies, such that the deformation of a filament extended in the z direction is characterized simply by its cross-sectional area $A(z, t)$ and an area averaged z component of velocity $v(z, t)$.

A choice must then be made for how to model the no-slip condition where the sample ends meet the experimental endplates. A good approximation [35–37] for initial aspect ratios $\Lambda = L_0/R_0 \geq 1$ is to invoke a divergent viscosity over a small region of the filament near each plate, acting to pin the fluid to the plates. (Equivalently, this region can be thought of as *part* of the plates.) We adopt this assumption [29], and have checked that the physics reported is robust to it by also performing simulations (not shown) with periodic boundary conditions (corresponding to a stretched torus, without end plates).

We neglect surface tension, restricting to the development of a neck in a highly elastoplastic filament in which bulk stresses dominate. Clearly, surface tension must ultimately become important in the very final stages of breakup, once the radius becomes small [38]. However our focus is not on the details of that final pinch-off, but on the time at which necking first becomes appreciable, which we define as the center-point radius having fallen to 15% of the initial radius.

The basic phenomenon that we seek to explain is shown in Fig. 1. This displays the necked profiles of two filaments: one that has been drawn relatively slowly compared to the inverse age and another that has been drawn more quickly. As can be seen, the slowly drawn filament survives to a relatively longer draw ratio before approaching failure, and displays a gradual necking profile. In contrast, the rapidly

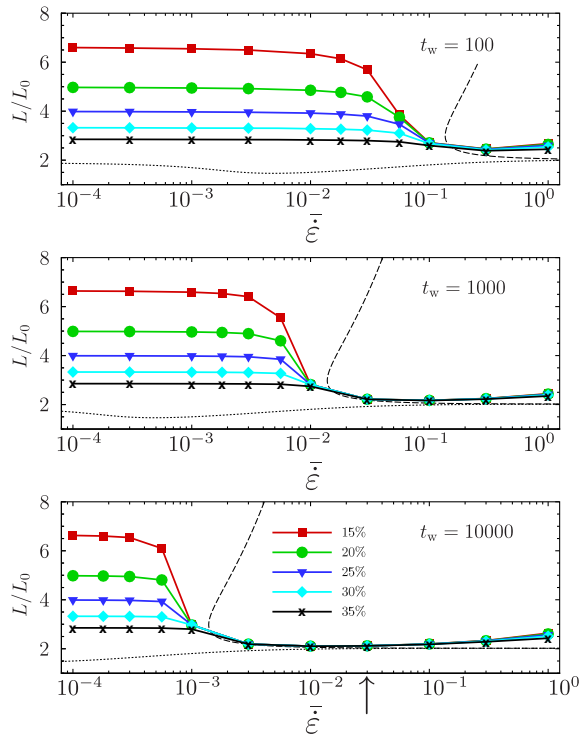


FIG. 2 (color online). Fluidity model in protocol (a). Solid lines: draw ratio at which the radius of the filament at its thinnest point has fallen to 35%, 30%, ..., 15% of the initial filament radius (curves upwards). Data are shown for three different initial sample ages (panels downwards). Initial aspect ratio $\Lambda = 2$. Dotted lines: Considère criterion [22]. Dashed lines: counterpart of the Considère criterion for elastoplastic materials. Parameters: $\mu = 0.1$ and $\eta = 0.01$. Arrow shows $\bar{\epsilon}$ for Fig. 1.

drawn filament fails sooner and with a more pronounced, cusplike profile.

That basic observation is quantified for the fluidity model in Fig. 2, for protocol (a) in which the Hencky strain rate $\bar{\epsilon}$ is held constant and the sample ends separate exponentially. The symbols show the draw ratio $L(t)/L_0$ at which appreciable necking becomes apparent, versus that applied strain rate. As can be seen, old samples ($\bar{\epsilon}t_w \gg 1$) fail at a modest draw ratio L/L_0 , while young samples ($\bar{\epsilon}t_w \ll 1$) survive to a larger L/L_0 . Also shown (dotted line) is the Considère criterion at which the tensile force first starts declining with strain. This would signal necking onset in a rate-independent solid but evidently performs badly here for young samples $\bar{\epsilon}t_w < O(1)$. We return below to discuss this in the context of an alternative criterion shown by the dashed lines. Figure 3 confirms the same behaviour in the SGR model. The same behaviour is also seen [29] in protocol (b), which has a constant drawing rate $\dot{L} = \bar{\epsilon}_0 L_0$ and progressively decreasing strain rate $\bar{\epsilon} = (1/\bar{\epsilon}_0 + t - t_w)^{-1}$.

To allow analytical insight, let us consider now a highly simplified, toy description of an elastoplastic filament in

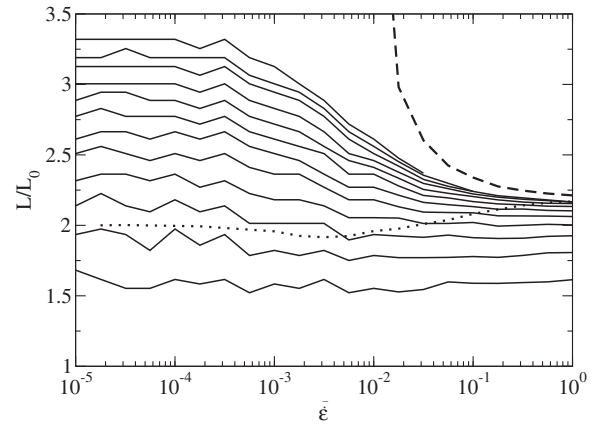


FIG. 3. SGR model in protocol (a). Solid contour lines upward show where initial area perturbations have increased in amplitude by successive powers of 1.4. The initial area profile was seeded such that $A = 1 + \xi \cos(2\pi u)$, where $\xi = 3 \times 10^{-4}$. Dotted line: Considère criterion. Dashed line: counterpart criterion for elastoplastic material. Parameters: $x = 0.3$, $\lambda = 1.5$, $t_w = 10^2$.

extensional deformation. The relevant dynamical quantities are the area profile $A(z, t)$, the z component of velocity $v(z, t)$, the strain rate field $\dot{\epsilon}(z, t) = \partial_z v(z, t)$, with the overall applied strain rate $\bar{\epsilon}(t) = \int_0^L dz \dot{\epsilon}(z, t)/L$, the elastoplastic stress $GZ(z, t)$, which we write as a constant modulus G times a strainlike variable Z , the total tensile stress $\sigma_E(z, t) = GZ + 3\eta\dot{\epsilon}$, and force $F(t) = \sigma_E A$.

These obey the conditions of mass and force balance:

$$\begin{aligned} \partial_t A + v \partial_z A &= -\dot{\epsilon} A \\ 0 &= \partial_z (A \sigma_E). \end{aligned} \quad (3)$$

We then choose for Z the simplest possible dynamics that combines elastic loading (f) and plastic relaxation (g):

$$\partial_t Z + v \partial_z Z = \dot{\epsilon} f(Z) - \frac{1}{\tau} g(Z). \quad (4)$$

We intentionally leave the forms of f and g unspecified, in order to derive below general instability criteria that do not depend on particular choices. For simplicity we do not include in this toy description explicit dynamics for τ , but below comment on predictions when $\bar{\epsilon}\tau \gg 1$ and $\bar{\epsilon}\tau \ll 1$, thereby inserting ageing $\tau \sim t_w$ “by hand.”

Within this toy model, we consider an initially near uniform cylindrical filament and express its state as the sum of a time-dependent uniform base state, corresponding to a perfect cylinder being stretched, plus small amplitude heterogeneous perturbations. Accordingly, we write $a(u, t) = \bar{a} + \delta a_q(t) \exp(iqu)$, $Z(t) = \bar{Z}(t) + \delta Z_q(t) \exp(iqu)$, $\dot{\epsilon}(u, t) = \bar{\epsilon}(t) + \delta \dot{\epsilon}_q(t) \exp(iqu)$, choosing for convenience to work in the coextending, cothinning frame by defining transformed length and area variables $u = z \exp(-\bar{\epsilon})$ and $a = A \exp(\bar{\epsilon})$. We then

perform a linear stability analysis to determine the time at which these heterogeneous perturbations start to grow, corresponding to the onset of necking. Substituting into Eqs. (3) and expanding in powers of the perturbation amplitude gives at first order

$$\partial_t \begin{pmatrix} \delta a \\ \delta Z \end{pmatrix}_q = \mathbf{M}_q(t) \cdot \begin{pmatrix} \delta a \\ \delta Z \end{pmatrix}_q, \quad (5)$$

in which the stability matrix \mathbf{M} has inherited the time dependence of the uniform base state.

At least one eigenvalue of \mathbf{M} being positive at any time t then gives a strong indication that the heterogeneous perturbations will be growing at that time, corresponding to the development of necking. (Direct integration of the linearised equations confirms this, and also agrees with the early-time growth of a neck in a full nonlinear solution.) In fact, it is straightforward to show that \mathbf{M}_q has two distinct modes of instability. One of these, which we call mode 1, has an eigenvalue of order $\bar{\epsilon}$ that is positive when the tensile stress of the underlying base state obeys $\bar{\epsilon}f' - (1/\tau)g' = \bar{\sigma}_E/\dot{\sigma}_E < 0$. It is liquidlike in the sense that its onset is determined by an interplay between elastic loading (specified by f) and plastic relaxation (via g). The other (mode 2) has a much larger eigenvalue of order G/η that is positive when the base state $\sigma_E - Gf > 0$; its onset condition is set only by the solidlike elastic loading term f , independent of g [39].

These analytics explain our numerical results in the SGR and fluidity models as follows. We indeed see a mode directly analogous to mode 1, the onset of which involves both the elastic loading and plastic relaxation dynamics, and which involves significant plastic relaxation along the entire filament. Its quantitative onset criterion is however modified compared with the toy model, due to the higher dynamical dimensionality of the full models: it is actually unstable for all strain rates and at all times during stretching. Any small perturbations to an initially cylindrical profile therefore start slowly growing as soon as stretching starts, for all strain rates. It is this mode that eventually leads to failure at relatively large L/L_0 for young samples $\bar{\epsilon}t_w \ll 1$ in Figs. 2 and 3.

For old samples, the solidlike mode 2 intervenes to cause failure at smaller strains. Its onset criterion $\sigma_E - Gf > 0$ transcribes [once cast into the forms of Eqs. (7), (8) below] unmodified to the fluidity and SGR models (and indeed any model, however, complex). It is shown by the dashed line in Figs. 2 and 3, and is only satisfied if $\bar{\epsilon}\tau \gg 1$, i.e., in old samples for which $\bar{\epsilon}t_w \gg 1$. It is furthermore only met a finite time after the start of stretching. Once unstable, however, its much larger eigenvalue $O(G/\eta)$ gives much more rapid necking and the sample fails very shortly after instability onset, at only modest draw ratios. (This mode would, in principle, restabilize at higher strains, as seen in

Fig. 2 by the doubling back of the dashed line, but that is irrelevant because the filament will have failed by then.)

How do we understand this instability criterion, $\sigma_E - Gf > 0$ of mode 2? Noting that the tensile force $F = A\sigma_E$, we have (for the underlying base state)

$$\frac{\partial F}{\partial \epsilon} = A \left(-\sigma_E + \frac{\partial \sigma_E}{\partial \epsilon} \right) = A \left(-\sigma_E + Gf - G \frac{g}{\dot{\epsilon}\tau} \right). \quad (6)$$

This follows from Eqs. (3) and (4), neglecting terms $O(\eta/G)$. Were the Considère criterion to apply directly, that would give instability for $\sigma_E - Gf + Gg/\dot{\epsilon}\tau > 0$. However, the dotted lines in Figs. 2 and 3 show this criterion to perform poorly for young samples $\bar{\epsilon}t_w < O(1)$. We can, though, define a modified derivative,

$$\left. \frac{\partial F}{\partial \epsilon} \right|_{\text{elastic}} = A(-\sigma_E + Gf), \quad (7)$$

in which the plastic relaxation term is artificially switched off over the strain increment in question. We thereby recognize the onset of mode 2 instability as

$$\left. \frac{\partial F}{\partial \epsilon} \right|_{\text{elastic}} < 0. \quad (8)$$

It is this criterion that is marked as a dashed line in Figs. 2 and 3. It performs much better for these ageing materials, over the full range of $\bar{\epsilon}t_w$, than the original Considère criterion. It coincides with Considère only for $\bar{\epsilon}t_w \gg 1$: in this regime, the material behaves essentially as a nonlinear elastic solid (with $\dot{\epsilon}f \gg (g/\tau)$), at least until necking first arises. (Once appreciable necking occurs it causes plastic flow in the thinning, central region of the filament.) Accordingly, we propose Eq. (8) as the counterpart for rate-dependent elastoplastic materials of the Considère criterion for rate-independent solids.

Finally, we have checked that our results are robust to reasonable variations in the values of the initial aspect ratio Λ and the Newtonian viscosity η , and that they apply robustly over large regions of the space of the phenomenological parameters μ (fluidity) and λ, x (SGR, within its glass phase $x < 1$). See the Supplemental Material for details [29].

To summarize, we have shown the instability to necking of a filament of soft glassy material to proceed by one of two possible modes. Young samples neck gradually via a mode informed by both elastic loading and plastic relaxation. Old samples fail more suddenly via a mode in which onset is informed only by elastic loading, and which is the counterpart for elastoplastic materials of the Considère mode of rate-independent solids. A particularly appealing feature of the physical picture presented here is this cross-over between two distinct modes of instability, determined simply by the age of the sample relative to the inverse

stretching rate. Having shown this numerically in two widely used models of soft glasses, as well as analytically, we argue these predictions to apply generically to all ageing elastoplastic materials. Indeed they may apply even more generally still, to pasty materials with long relaxation time scales τ but much weaker ageing effects, now set by the value of the inverse strain rate relative to τ . It remains an open challenge to understand how, within SGR, these ductile failure modes cross over to brittle cracking at even higher strain rates, for samples with notchlike initial imperfections [40,41].

The research leading to these results has received funding from the European Research Council under the European Union's Seventh Framework Programme (FP7/2007-2013) / ERC Grant Agreement No. 279365.

*Corresponding author.

suzanne.fielding@durham.ac.uk

- [1] S. M. Fielding, P. Sollich, and M. E. Cates, *J. Rheol.* **44**, 323 (2000).
- [2] L. C. E. Struik, *Physical Aging in Amorphous Polymers and Other Materials* (Elsevier, Houston, 1978).
- [3] H. S. Chen, *Rep. Prog. Phys.* **43**, 353 (1980).
- [4] F. M. Huisman, S. R. Friedman, and P. Taborek, *Soft Matter* **8**, 6767 (2012).
- [5] N. Niedzwiedz, H. Buggisch, and N. Willenbacher, *Rheol. Acta* **49**, 1103 (2010).
- [6] S. R. Derkach, *Adv. Colloid Interface Sci.* **151**, 1 (2009).
- [7] E. Miller, C. Clasen, and J. P. Rothstein, *Rheol. Acta* **48**, 625 (2009).
- [8] P. Coussot and F. Gaulard, *Phys. Rev. E* **72**, 031409 (2005).
- [9] A. Shaukat, A. Sharma, and Y. Joshi, *Rheol. Acta* **49**, 1093 (2010).
- [10] A. Shaukat, M. Kaushal, A. Sharma, and Y. M. Joshi, *Soft Matter* **8**, 10107 (2012).
- [11] M. Arciniaga, C.-C. Kuo, and M. Dennin, *Colloids Surf. A* **382**, 36 (2011).
- [12] C.-C. Kuo and M. Dennin, *J. Rheol.* **56**, 527 (2012).
- [13] C.-C. Kuo and M. Dennin, *Phys. Rev. E* **87**, 052308 (2013).
- [14] H.-N. Lee, K. Paeng, S. F. Swallen, and M. D. Ediger, *Science* **323**, 231 (2009).
- [15] J. Rottler, *J. Phys. Condens. Matter* **21**, 463101 (2009).
- [16] L. O. Eastgate, J. S. Langer, and L. Pechenik, *Phys. Rev. Lett.* **90**, 045506 (2003).
- [17] C. H. Rycroft and F. Gibou, *J. Comput. Phys.* **231**, 2155 (2012).
- [18] P. J. Zimoch, G. H. McKinley, and A. E. Hosoi, *Phys. Rev. Lett.* **111**, 036001 (2013).
- [19] M. Roché, H. Kellay, and H. A. Stone, *Phys. Rev. Lett.* **107**, 134503 (2011).
- [20] M. I. Smith, R. Besseling, M. E. Cates, and V. Bertola, *Nat. Commun.* **1**, 114 (2010).
- [21] M. Chellamuthu, E. M. Arndt, and J. P. Rothstein, *Soft Matter* **5**, 2117 (2009).
- [22] M. Considère, *Ann. Ponts Chaussees* **9**, 574 (1885).
- [23] J. W. Hutchinson and K. W. Neale, *Acta Metall.* **25**, 839 (1977).
- [24] Note, however, related work on dependence on age (via initial condition) of crack propagation from a notch [41].
- [25] P. Sollich, F. Lequeux, P. Hebraud, and M. E. Cates, *Phys. Rev. Lett.* **78**, 2020 (1997).
- [26] M. E. Cates and P. Sollich, *J. Rheol.* **48**, 193 (2004).
- [27] M. Doi and T. Ohta, *J. Chem. Phys.* **95**, 1242 (1991).
- [28] S. M. Fielding, M. E. Cates, and P. Sollich, *Soft Matter* **5**, 2378 (2009).
- [29] See Supplemental Material at <http://link.aps.org/supplemental/10.1103/PhysRevLett.114.158301> for a description of the one dimensional approximation, transformation to coextending and cothinning reference frame, no-slip boundary condition, and results for the constant velocity protocol. We also discuss the robustness to variations in the parameter choices made in the main text.
- [30] M. M. Denn, C. J. S. Petrie, and P. Avenas, *AIChE J.* **21**, 791 (1975).
- [31] D. O. Olagunju, *J. Non-Newtonian Fluid Mech.* **87**, 27 (1999).
- [32] M. Yao and G. H. McKinley, *J. Non-Newtonian Fluid Mech.* **74**, 47 (1998).
- [33] M. Tembely, D. C. Vadillo, M. R. Mackley, and A. Soucemarianadin, *J. Rheol.* **56**, 159 (2012).
- [34] D. C. Vadillo, M. Tembely, N. F. Morrison, O. G. Harlen, M. R. Mackley, and A. Soucemarianadin, *J. Rheol.* **56**, 1491 (2012).
- [35] Y. M. Stokes, E. O. Tuck, and L. W. Schwartz, *Q. J. Mech. Appl. Math.* **53**, 565 (2000).
- [36] C. Clasen, J. Eggers, M. A. Fontelos, J. Li, and G. H. McKinley, *J. Fluid Mech.* **556**, 283 (2006).
- [37] P. Szabo, G. H. McKinley, and C. Clasen, *J. Non-Newtonian Fluid Mech.* **169–170**, 26 (2012).
- [38] The contributions to force balance of the viscoelastic stresses and surface tension are, respectively, $G\partial_z\Sigma$ and (at leading order) $\gamma\partial_z R^{-1}$ where γ is the coefficient of surface tension and R the radius of the filament.
- [39] Constitutive models that are too oversimplified to address the physics soft glasses, such as the Oldroyd B model, have an elastic loading term of trivially simple form and this mode 2 instability criterion is never met.
- [40] M. L. Falk, *Phys. Rev. B* **60**, 7062 (1999).
- [41] C. H. Rycroft and E. Bouchbinder, *Phys. Rev. Lett.* **109**, 194301 (2012).